



## Post irradiation examination of thermal reactor fuels

D.N. Sah<sup>a,\*</sup>, U.K. Viswanathan<sup>b</sup>, E. Ramadasan<sup>b</sup>, K. Unnikrishnan<sup>b</sup>, S. Anantharaman<sup>b</sup>

<sup>a</sup> Raja Ramanna Fellow, Post Irradiation Examination Division, Bhabha Atomic Research Centre, Trombay, Mumbai 400 085, India

<sup>b</sup> Post Irradiation Examination Division, Bhabha Atomic Research Centre, Trombay, Mumbai 400 085, India

### ARTICLE INFO

PACS:  
81.40Wx

### ABSTRACT

The post irradiation examination (PIE) facility at the Bhabha Atomic Research Centre (BARC) has been in operation for more than three decades. Over these years this facility has been utilized for examination of experimental fuel pins and fuels from commercial power reactors operating in India. In a program to assess the performance of (U,Pu)O<sub>2</sub> MOX fuel prior to its introduction in commercial reactors, three experimental MOX fuel clusters irradiated in the pressurized water loop (PWL) of CIRUS up to burnup of 16000 MWd/tU were examined. Fission gas release from these pins was measured by puncture test. Some of these fuel pins in the cluster contained controlled porosity pellets, low temperature sintered (LTS) pellets, large grain size pellets and annular pellets. PIE has also been carried out on natural UO<sub>2</sub> fuel bundles from Indian PHWRs, which included two high burnup (~15000 MWd/tU) bundles. Salient investigations carried out consisted of visual examination, leak testing, axial gamma scanning, fission gas analysis, microstructural examination of fuel and cladding,  $\beta$ ,  $\gamma$  autoradiography of the fuel cross-section and fuel central temperature estimation from restructuring. A ThO<sub>2</sub> fuel bundle irradiated in Kakrapar Atomic Power Station (KAPS) up to a nominal fuel burnup of ~11000 MWd/tTh was also examined to evaluate its in-pile performance. The performance of the BWR fuel pins of Tarapur Atomic Power Stations (TAPS) was earlier assessed by carrying out PIE on 18 fuel elements selected from eight fuel assemblies irradiated in the two reactors. The burnup of these fuel elements varied from 5000 to 29000 MWd/tU. This paper provides a brief review of some of the fuels examined and the results obtained on the performance of natural UO<sub>2</sub>, enriched UO<sub>2</sub>, MOX, and ThO<sub>2</sub> fuels.

© 2008 Elsevier B.V. All rights reserved.

### 1. Introduction

Reliable performance of nuclear fuels has a large bearing on economics of nuclear power and radiation safety of plant operating personnel. Fuel performance in the reactor is, therefore, routinely monitored. On selected fuel bundles discharged from the reactor, PIE is periodically carried out to generate feedback information which is used by the fuel designer, fuel fabricator and the reactor operator to bring about changes for improved performance of the fuel. In the last three decades, post irradiation examination of different types of experimental as well as power reactor fuels has been carried out in the hot cells facility of the Post Irradiation Examination Division of BARC. This paper presents the salient findings on fuels examined.

### 2. Hot cells facility and investigations

The PIE facility consists of six concrete shielded hot cells, capable of handling activities varying from 10<sup>2</sup> Curies to 10<sup>5</sup> Curies of

1.3 MeV gamma radiation [1,2]. A scanning wall-periscope with a magnification of 10× is provided for visual examination. The fuel for PIE is loaded into the first cell through a shielded transfer system. The as-received fuel assembly is examined visually using the cell windows and the wall periscope. The fuel bundle is then dismantled to separate the fuel elements. The separated elements are examined visually to ensure that all the welded appendages are intact and also for the presence of surface defect like cracks, corrosion, discoloration, fretting, ridging etc. The fuel element is moved in front of a collimator fitted in the front wall of the cell and the axial gamma activity profile of the element is obtained by gamma scanning, using a gamma spectrometer. The axial diameter profile of the fuel element is obtained by using a profilometer. The defect inside the clad or in the end cap welds is located by scanning the fuel element by using ultrasonic probes. Apparently intact fuel elements are then taken up for leak testing using the liquid nitrogen–alcohol method. After the leak test, the fuel elements are punctured for the measurement of released fission gases. The quantitative estimation of the released gases is carried out by applying the law of gas mixtures by measuring the gas pressure using capacitance diaphragm gauge and the elemental and isotopic estimation by using a dual column gas chromatograph and a quadrupole mass analyser. Microstructural examination is

\* Corresponding author. Tel.: +91 22 2559 5009; fax: +91 22 2550 5151.  
E-mail address: [dnsah@barc.gov.in](mailto:dnsah@barc.gov.in) (D.N. Sah).

**Table 1**  
List of fuels examined

Sl. no.	Type of fuel	No. of fuel clusters/bundles/elements	Burnup (MWd/tU)
1	MOX (UO <sub>2</sub> -4% PuO <sub>2</sub> )	3 clusters	2000–16000
2	PHWR–Natural UO <sub>2</sub>	5 bundles	390–15000
3	PHWR–ThO <sub>2</sub>	2 bundles	11 000–15 000
4	BWR–enriched UO <sub>2</sub>	18 elements	5000–29000

carried out on transverse and longitudinal sections taken from region of interest in the fuel elements. The mechanical properties of the cladding are estimated by carrying out ring-tension tests on the sectioned clad tubes, after removing the fuel.

### 3. Fuels examined

Table 1 gives the list of fuels examined from different sources, along with their average discharge burnup. The main aim of PIE

of experimental MOX fuel was to assure the satisfactory performance of this fuel before its introduction in the BWRs. A typical experimental MOX fuel pin is shown in Fig. 1(a) and the cluster geometries used for the irradiation experiments are shown in Fig. 1(b). MOX clusters, contained UO<sub>2</sub> + 4% PuO<sub>2</sub> fuel in Zircaloy-2 free standing cladding [3]. Cluster AC2 and AC3 were irradiated to a nominal burnup of 16000 MWd/tU. The peak linear heat rating during irradiation in AC2 and AC3 had been estimated to be 414 W/cm and 490 W/cm, respectively. Another experimental 2-tier cluster AC4 consisted of six fuel elements with a number of variables such as varying pellet-clad gap, annular pellets, Ar & He mixture as filler gas and pellets manufactured through the low temperature sintering (LTS) route. The cluster was irradiated to 2000 MWd/tU, at a linear heating rate of 490 W/cm.

PHWR fuel bundles were the standard 19-element fuel assemblies of natural UO<sub>2</sub> or ThO<sub>2</sub> fuel, clad in 0.4 mm thick collapsible Zircaloy-2 tubes. Details of a typical 19-element fuel assembly are shown in Fig. 2. PIE was carried out on the PHWR fuel pins from two high burnup UO<sub>2</sub> fuel bundles, irradiated to a nominal burnup of 15000 MWd/tU. A few low burnup UO<sub>2</sub> fuel bundles and one ThO<sub>2</sub> fuel bundle irradiated to a nominal burnup of 11000 MWd/tU, were also examined. The main aim of the examination was

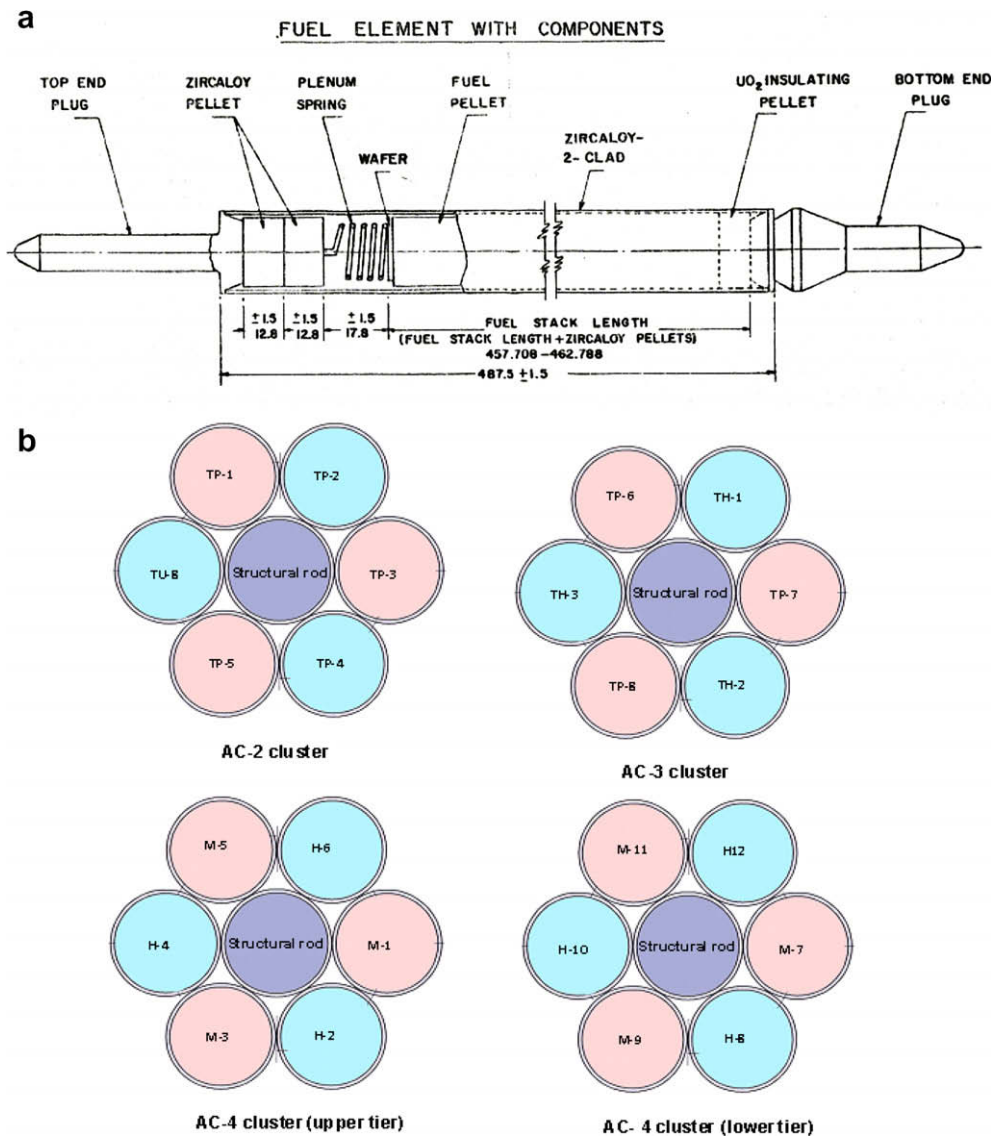


**Fig. 1.** (a) A typical experimental fuel pin used for MOX irradiation. (b) Typical cluster assemblies used for MOX irradiation.

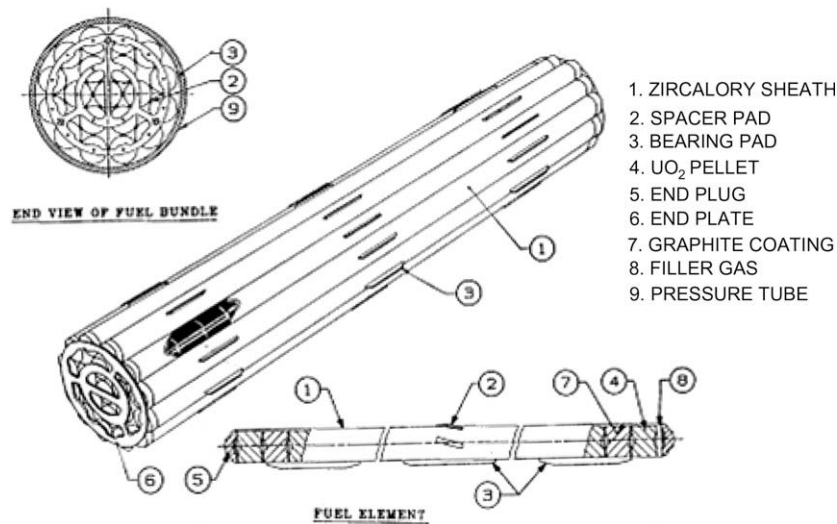


Fig. 2. Details of 19-pin PHWR fuel bundle.

to identify the main causes of failures in low burnup fuels and to assess the performance of PHWR fuel at extended burnup with respect to corrosion, pellet clad interaction (PCI) and fission gas release. Examination included visual examination, gamma scanning, fission gas release, metallography and autoradiography.

Eighteen BWR fuel elements from Tarapur Atomic Power Station (TAPS) were selected for PIE, from eight fuel assemblies having a burnup in the range of 5000–29000 MWd/tU. The investigations included measurement of axial burnup profile, fission gas release, examination of uniform and nodular corrosion on cladding surface, mechanical testing of cladding, SEM/EPMA examination of clad inside surface, metallography of fuel and cladding and beta–gamma autoradiography to study fission product redistribution. Fuel temperature was estimated using restructuring observed in the fuel.

## 4. Results and discussion

### 4.1. MOX fuel clusters [3,4]

No abnormal corrosion, deformation or ridging was observed during visual examination of MOX fuel pins. Leak testing confirmed that none of the irradiated fuel elements had failed. Fission gas measurements were carried out on MOX fuel pins and results are given in Table 2. The average burnup of the fuel, peak linear

heat rating, fuel pin number and the percentage of fission gas released are given in the table. All the MOX fuel pins of cluster AC2 showed <1% fission gas release (FGR) and did not show any increase in the internal pressure. The fission gas release in the fuel pins of cluster AC3 was 8–10% due to higher linear heat rating and the measured internal pressures were in the range of 7–8 atmospheres.

The fission gas release in the fuel pins of cluster AC4 depended on the design. The fuel elements AC4 M3 and AC4 M7 contained annular pellets. Filler gas in AC4 M3 was helium. AC4 M7 was filled with a mixture of 10% He and Ar to simulate the effects of lower gap conductance. Both of the fuel elements containing annular pellets did not release any gas. The fuel element AC4 M9, which contained regular chamfered cylindrical pellets, had released 3.2% of the gases generated. The measured internal pressures in the above pins were less than 3 atmospheres. AC4 M11 containing pellets manufactured through LTS route indicated a high release of 39% of the gases and the measured internal pressure was 4.5 atmospheres. The chromatogram of the released gases showed an unexpected peak, which was identified as due to the presence of carbon monoxide. Pre-irradiation documentation of the pellets indicated a higher impurity level of carbon in the pellets compared to the pellets in other pins, though well below the maximum allowed level. Zinc behenate is used as the binder, during pressing of the pellets. It appears that the CO formed during the oxidizing atmosphere, got entrapped in the pores during the early stages of sintering (LTS route), which subsequently might have been released during irradiation.

### 4.2. PHWR fuel

#### 4.2.1. High burnup bundle [5]

Results from one of the two high burnup fuels are discussed in this paper. The bundle was of the standard 19-element design with natural UO<sub>2</sub> fuel, clad in Zircaloy-2 (Fig. 2). The linear power ratings of the fuel pins in the outer ring, in the intermediate ring and the central fuel pin of the bundle are given as a function of burnup in Fig. 3. The fuel bundle examined in this study had attained an average burnup of 15000 MWd/tU, which is more than twice the designed discharge burnup of 7000 MWd/tU. The burnup in the peak rated fuel pins of outer ring, intermediate ring and the central pin were 15460 MWd/tU, 13120 MWd/tU and 12390 MWd/tU, respectively. Visual examination and leak testing showed

Table 2  
Fission gas release data from MOX clusters

MOX cluster	Average burnup (MWd/tU)	Peak linear heat rating (W/cm)	Fuel pin No.	Fission gas release (%)
AC2	16265	414	TU8	0
			TP1	0.1
			TP 2	0.1
			TP 3	0
			TP4	0.2
AC3	16000	490	TP5	0.4
			TP6	8.4
			TP7	10.5
			TP8	9.2
AC4	2000	490	M 1	0.1
			M 3	0
			M 5	0.3
			M 7	0
			M 9	3.2
			M 11	39.0

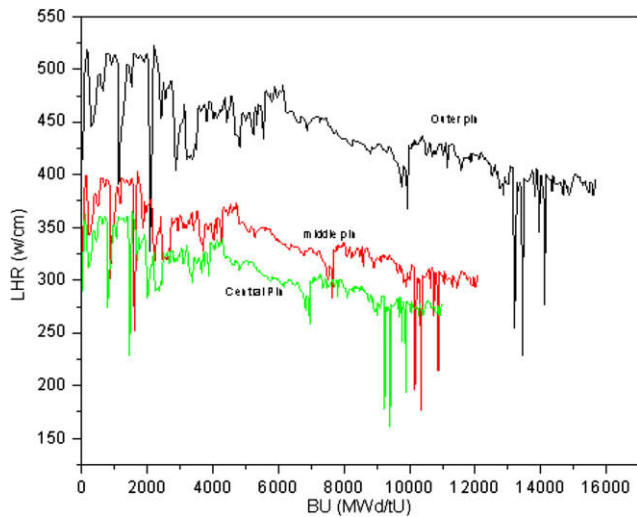


Fig. 3. Power history of fuel pins in bundle 56504.

that all the 19 fuel pins of the bundle were intact, demonstrating that PHWR fuel pins can operate up to such high burn ups, without failure, under normal operating conditions.

**4.2.1.1. Fission gas release.** The results of fission gas release measurement on five outer ring fuel pins, two intermediate ring fuel pins and the central fuel pin in the bundle are given in Table 3. The measured internal gas pressure in the five outer fuel pins was in the range 21–28 bar. The corresponding pressures in the central and intermediate fuel pins were 3.2 and 4.4 bar, respectively. The fission gas release fraction in the outer fuel pins was in the range of 19–22%. The fractions in the intermediate and central pin were 2% and <1%, respectively. The observed higher gas release in the outer fuel pins is due to their higher power rating and the higher burnup as compared to that of the intermediate and central pins. Increased gas release at high burnup is of concern, since it leads to high internal gas pressure in the outer pin. Since the void volume available in the pin is very small, there is the possibility of internal gas pressure in the fuel pin exceeding the external coolant pressure during off normal operation at the burnup of this magnitude. This may lead to clad lift-off, resulting in unacceptable changes in the pin diameter. However, no abnormal increase in the diameter was observed during the PIE of the fuel pins from this bundle.

**4.2.1.2. Macrostructure.** Macrostructural examination of the fuel cross-section taken from different axial locations in the fuel pin from the outer ring of the bundle was carried out. A central dark

porous region extending up to a fuel fractional radius of about 0.55 was observed in all the sections. A typical macrostructure of one of the samples from the axial location is shown in Fig. 4. A circumferential crack existed adjacent to the boundary of the dark region. Observation of the dark porous region at higher magnification revealed interconnected pores/bubbles on the grain boundaries (Fig. 5). White particles, probably noble fission products, were also observed in the microstructure. The size of dark porous region in the intermediate and central fuel pins was much smaller than the size in the outer fuel pin.

The crevice region around the spot weld between the clad and the bearing pad of the outer pin is shown in Fig. 6. There was no evidence of localized accelerated corrosion at this location. The average oxide layer thickness was 2.7  $\mu\text{m}$ .

$\beta$ - $\gamma$  autoradiography of samples from outer, intermediate and central pins was carried out on the metallographically polished

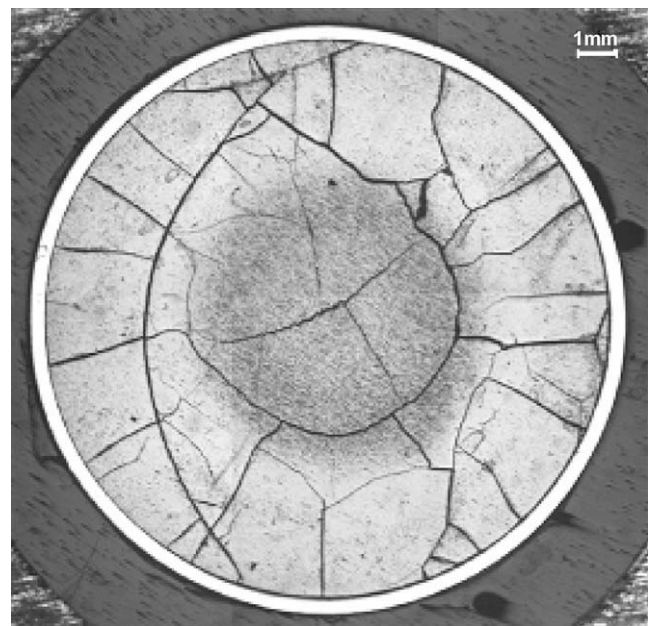


Fig. 4. A typical photomicrograph from the cross-section from the outer pin of the high burnup bundle.

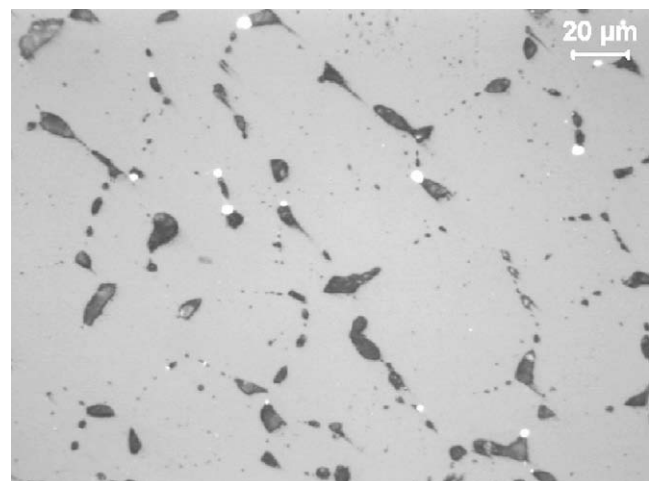


Fig. 5. Grain boundary bubbles at the centre of the fuel section of the outer pin of the high burnup bundle.

**Table 3**  
Fission gas release in high burnup PHWR fuel pins

Fuel pin	Xe/Kr ratio	Void volume ( $\text{cm}^3$ )	Internal pressure at ambient temperature (bar)	Volume of released fission gas at STP ( $\text{cm}^3$ )	Fission gas released (%)
Outer	12.1	3.1	27.6	74.9	22.2
Outer	12.0	3.1	25.7	69.2	20.5
Outer	12.1	3.3	23.7	65.6	19.4
Outer	12.1	3.6	1.4	65.2	19.3
Outer	12.1	3.7	24.0	74.2	22.0
Intermediate	7.8	3.0	4.4	5.0	1.7
Intermediate	7.7	3.3	4.2	6.1	2.1
Central	8.4	3.2	3.2	1.9	0.7

samples. The autoradiographs of samples are shown in Fig. 7(a–c). The central white region in the autoradiograph indicates that the radioactive fission products had migrated from the central region towards the periphery of the fuel section, resulting in lower activity in the central region and a higher activity in the outer region of the fuel cross-section. The radius of the central white region was maximum in case of the outer pin and was minimum for the central pin.

4.2.1.3. Fuel central temperature. The temperature distribution in fuel was estimated using the well-known  $\int K dT$  equation [6,7].

$$\int_{T_s}^{T_r} KdT = \frac{q}{4\pi} [1 - (r/R)^2] \quad (1)$$

where,  $K$  is the thermal conductivity, W/cm/°C, taken as a function of temperature

- $q$  is the linear heat rating (W/cm)
- $T_r$  is the temperature at radial position “ $r$ ” (°C)
- $T_s$  is the fuel surface temperature (°C)
- $r/R$  is the fractional fuel radius

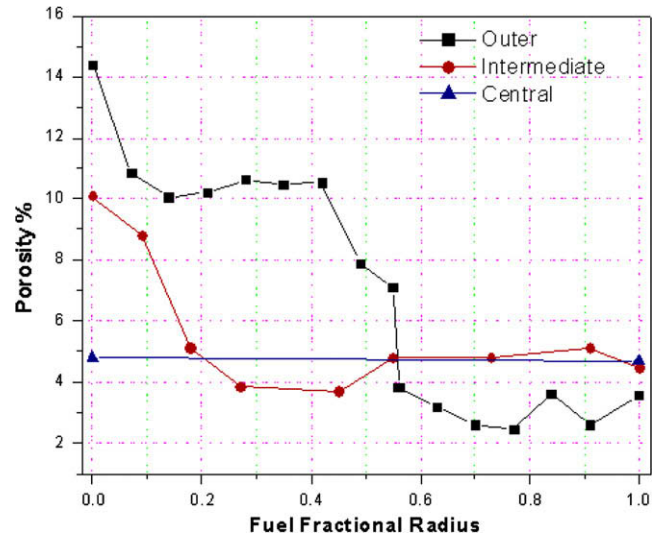


Fig. 8. Radial porosity profile of pellets from the outer, intermediate and the central pins of the high burnup bundle.

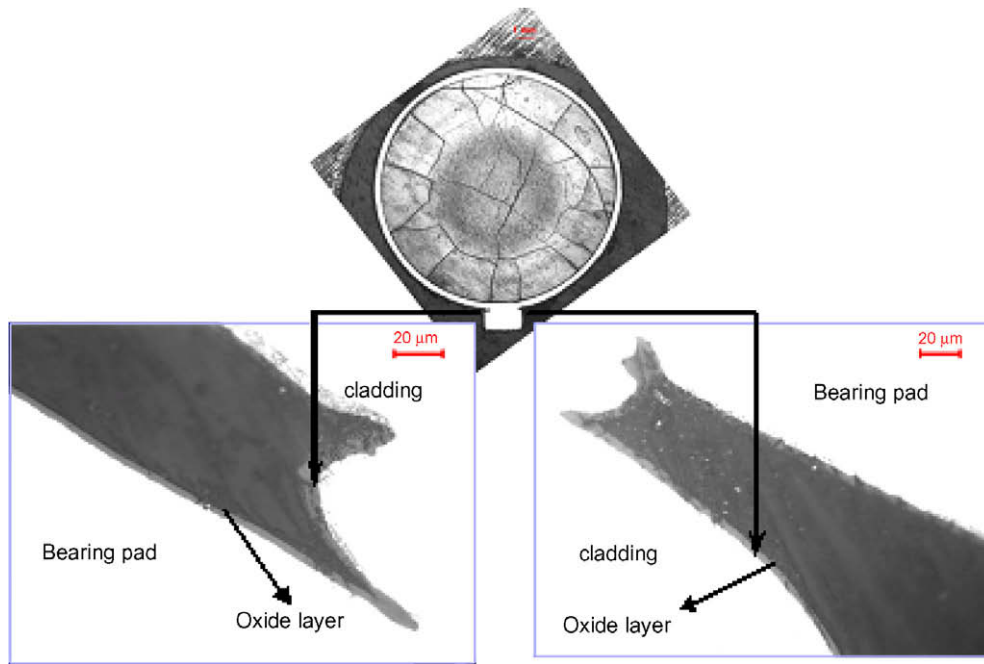


Fig. 6. Uniform corrosion at the crevice of the bearing pad of the outer pin of the high burnup bundle.

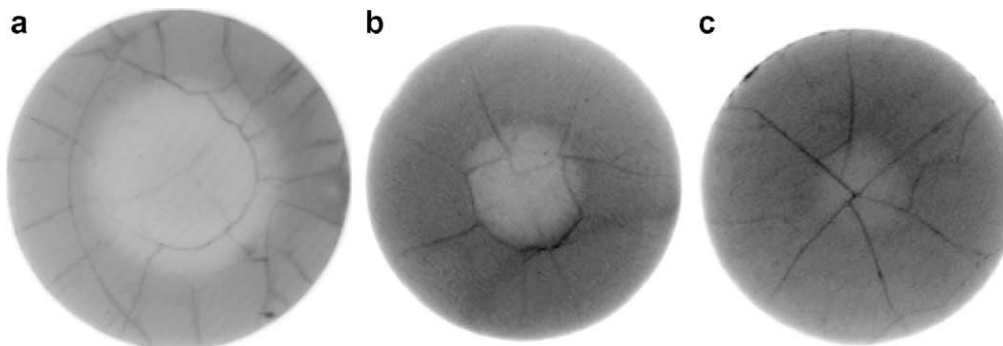


Fig. 7.  $\beta$ - $\gamma$  autoradiographs of (a) outer, (b) intermediate and (c) central pin of the high burnup bundle.

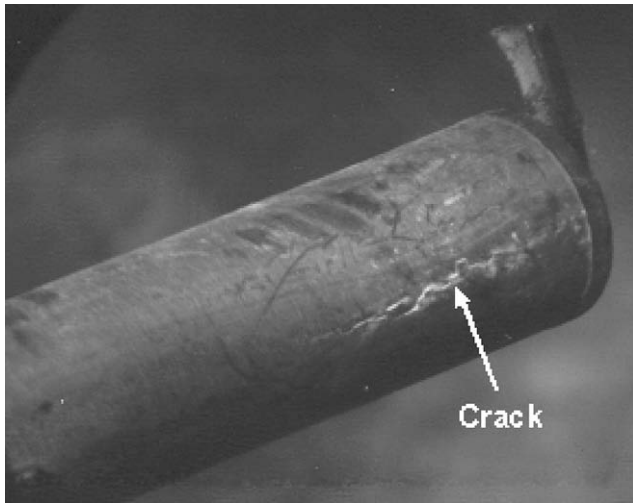


Fig. 9. Crack observed on the cladding of the outer fuel element of the low burnup bundle.

The temperature at a specific radial position in the fuel cross-section is inferred from the restructuring observed in the microstructure of the irradiated fuel. The regions of the onset of equiaxed grain growth and the appearance of intergranular porosity are taken as temperature markers. The temperature for the onset of equiaxed grain growth is taken as 1300 °C and temperature for the onset of intergranular porosity is taken as 1120 °C for fuel burnup of 10000–15000 MWd/tU [7]. The estimated centre temperatures of the outer, intermediate and central fuel pin were found to be 1700 °C, 1250 °C, and 1170 °C, respectively. The estimated central temperatures of the elements are in the order of their linear power rating in the PHWR fuel bundle. The outer elements operate at the highest linear power rating followed by the intermediate and the central elements. It may be mentioned that the fuel temperature estimated from restructuring represents the maximum temperature attained by the fuel during irradiation. The estimated temperature may have an error of  $\pm 5\%$  for the steady state operation of the fuel. The higher fission gas release observed in the outer

fuel pins could have been caused by high temperature mechanisms operating in the fuel like diffusion and grain boundary sweeping [8]. This could also be inferred from the higher Xe/Kr ratio observed in the fission gas collected from the outer elements. The higher Xe content could be due to higher rate of its diffusion in the outer elements.

**4.2.1.4. Fuel swelling.** The pellet average total porosity volume was estimated from the radial distribution of porosity in the pellet. The porosity measurement was carried out on as-polished metallographic samples using image analysis technique. Measured radial porosity profiles in the pellets are given in Fig. 8. Swelling was taken as the difference between total porosity in the irradiated fuel and the initial porosity. Based on the measured density values of as-fabricated fuel pellets the initial fuel porosity was estimated to be 3.7%. The estimated values of fuel swelling were 1.5%, 1.0% and 1.1%, respectively, in the outer, intermediate and central fuel pins. This shows a volumetric swelling rate of roughly 1% per 10000 MWd/tU.

**4.2.1.5. Fuel-clad interaction.** Examination of fuel sections did not indicate any interaction between fuel and cladding in the fuel pins. Though, a thick oxide layer of 4–5  $\mu\text{m}$  was observed on the inner surface of the cladding in the case of the outer fuel elements, no localised chemical interaction or fuel-clad bonding was observed. The measured fuel clad gap was 26  $\mu\text{m}$  in the outer pin, 24  $\mu\text{m}$  in the intermediate and 16  $\mu\text{m}$  in the central pins. The as-fabricated fuel-clad gap in the PHWR fuel element is about 40  $\mu\text{m}$ . The initial fuel-clad gap changes during irradiation due to a combined effect of fuel swelling which reduces the gap, and outward creep of the cladding which increases the gap. Measured fuel-clad gap was higher in case of the outer fuel pin and the intermediate fuel pins compared to that of the central fuel pin. This could be due to higher diametral creep of cladding tube in the outer and the intermediate pins than that in the central pin. The high fuel temperature results in large thermal expansion of the fuel. Due to large thermal expansion of the fuel the cladding will be subjected to tensile hoop stress, which causes outward creep of the cladding. The extent of outward creep is more in the outer and intermediate fuel pins due to higher fuel temperature.

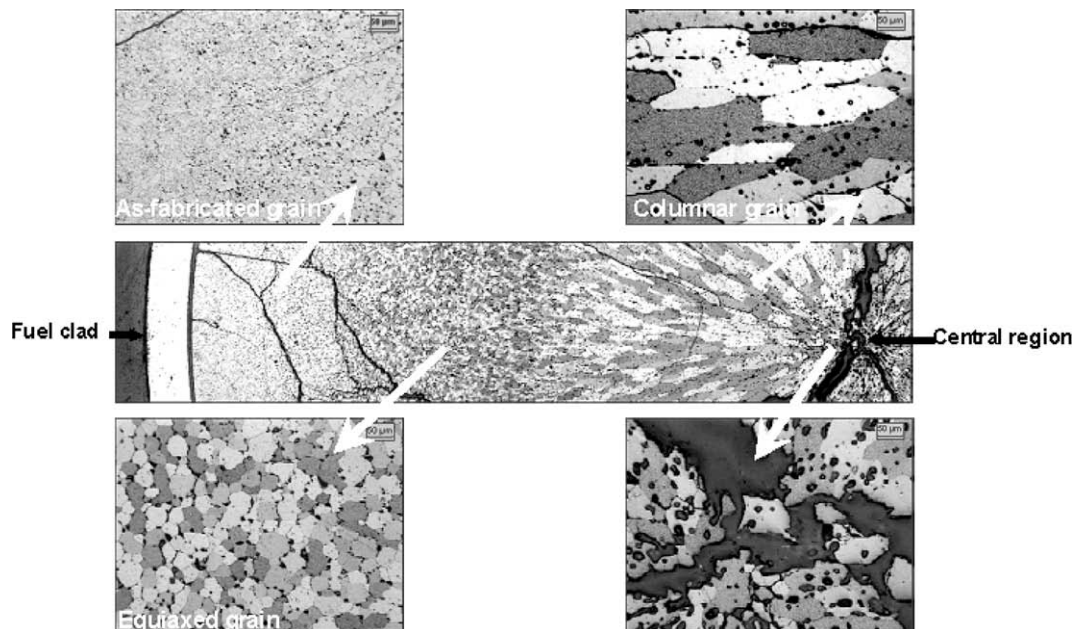


Fig. 10. Restructured zones from periphery to the centre of the fuel pellet in the failed pin at the location of failure of the low burnup bundle.

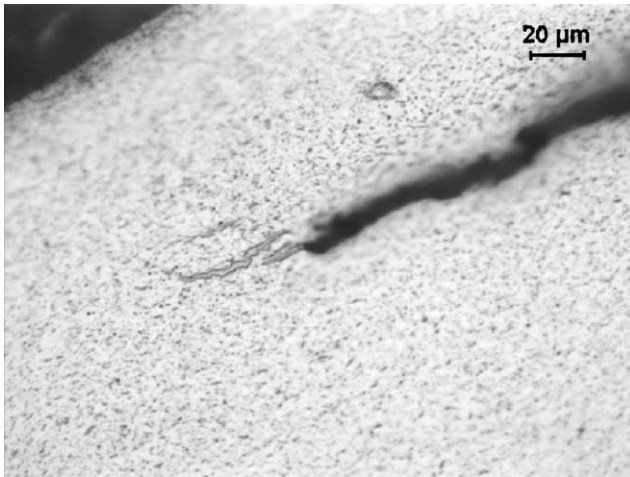


Fig. 11. Hydride platelet at the crack tips in the clad.

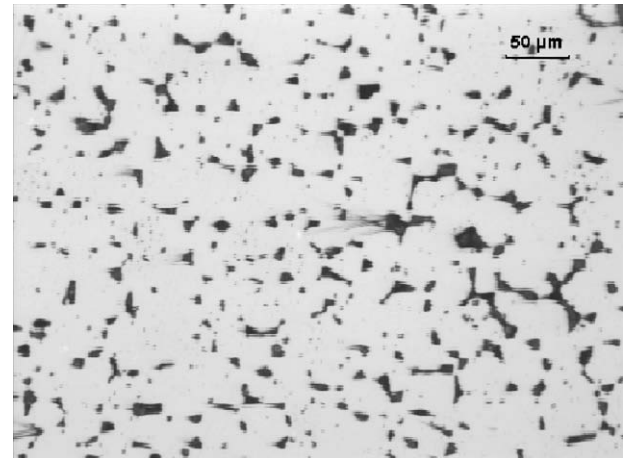


Fig. 13. Microstructure of the fuel cross-section in the un-failed adjacent pin.

#### 4.2.2. Low burnup bundles [9]

Examination of several failed fuel bundles at low burnups was carried out to identify the causes. Examination has revealed three main reasons for failures namely defect in the end cap weld, hydriding and fretting. An interesting failure was noticed in a fuel bundle at a burnup of 387 MWd/tU within 17 days of residence of the fuel bundle in the reactor. Leak testing of fuel pins after dismantling of the bundle showed that two of the 12 fuel pins in the outer ring had failures in the form of axial cracks slightly away from the end plug weld. The other fuel pins in the bundle were intact. Fig. 9 shows cracks observed in one of the failed fuel pins.

One of the failed fuel pins was sectioned at several places along the failed region and metallography was carried out. It can be seen from the photomicrograph (Fig. 10) that the fuel had undergone extensive restructuring resulting in the formation of columnar grains in the central region of the fuel pellet section. Based on the restructuring, the fuel centre temperature at the location of failure was estimated to be 2100 °C. Many incipient cracks were observed in the cladding, in addition to through wall cracks. Some of these cracks were in line with the radial cracks in the fuel. Hydride precipitates were found at the tip of the incipient cracks, as shown in Fig. 11. Cracks in the cladding were filled with an interaction product. The fuel was found to be in contact with the clad at several places along the circumference, indicating a strong interac-

tion with each other. Tell-tale features of the pellet-clad interaction/stress corrosion cracking (PCI/SCC) type of failure could be observed at several locations. But the fuel burnup was too low to provide sufficient inventory of iodine to promote SCC. Presence of hydride precipitates at the tip of incipient cracks, (Fig. 11), indicated crack propagation by progressive precipitation and cracking of hydrides at the crack tip.

In order to infer the thermal condition of the non-failed fuel pin in the outer ring, sections taken from the intact fuel pins were examined metallographically. A comparison of the photo macrographs of the sections of failed and unfailed fuel pins (Fig. 12) revealed that there was no visible fuel restructuring in the intact fuel pin (Fig. 12(a)), while the failed fuel pin showed extensive restructuring, as shown in Fig. 12(b). An examination of fuel at higher magnification revealed a microstructure of fuel containing intergranular pores at the fuel centre (Fig. 13), but no grain growth. Based on the microstructure, the fuel centre temperature in the intact fuel pin was estimated to be less than 1300 °C. Thus it was clear that the fuel centre temperature in the failed fuel pins was 800 °C higher than the fuel temperature in the intact fuel pins of outer ring during irradiation. As all the outer ring fuel pins experience identical heat ratings during operation, the cause of higher fuel temperature in the failed fuel pin was not clear.

The end plug portion of the failed fuel pin was subjected to ultrasonic testing inside hot cells. The ultrasonic testing indicated

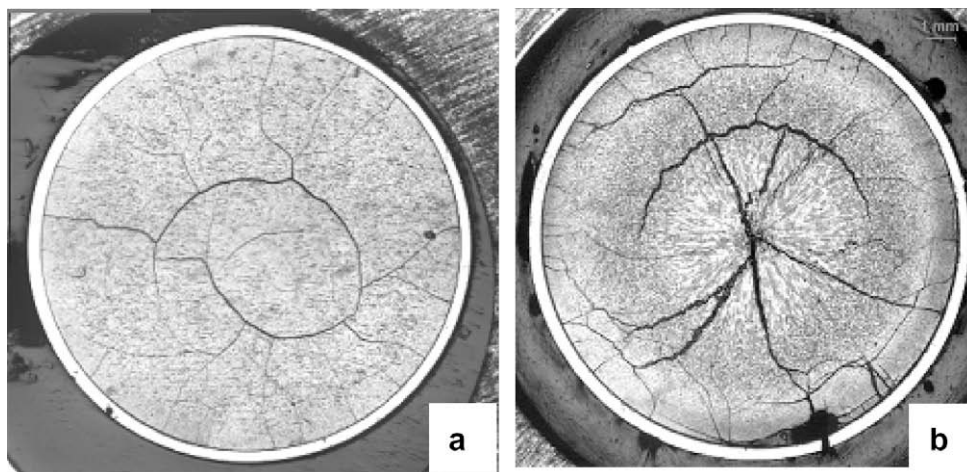


Fig. 12. Photo-macrograph of the fuel cross-section of (a) an un-failed adjacent pin and (b) failed pin.

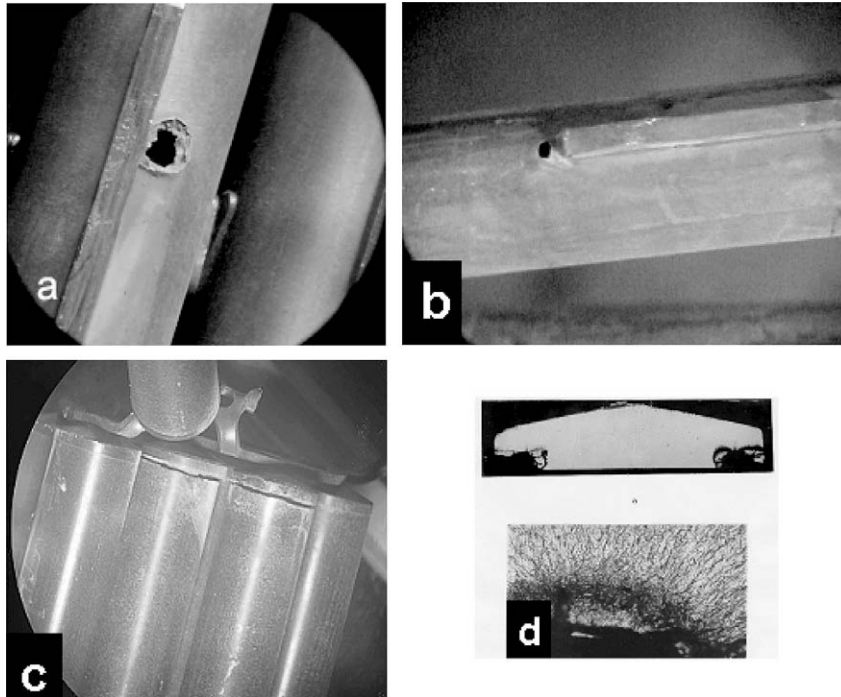


Fig. 14. (a) Pin hole in the clad due to hydride blister, (b) pin hole due to bearing pad damage, (c) cracks at the end plugs and (d) hydridding at the end plug.

presence of a lack-of-fusion type defect in the end plug weld of the fuel pin. Based on this, the cause of failure has been identified as the lack-of-fusion defect in the end cap weld of this pin, which might have gone undetected during the manufacture of the element. This defect had opened up during the reactor operation leading to the ingress of water in this pin. The presence of steam in the fuel-clad gap would have severely affected the gap-conductance, increasing the central temperature of the fuel. The presence of steam also caused the oxidation of  $\text{UO}_2$  with consequent reduction of fuel thermal conductivity and increase of fuel centre temperature. This led to an increased volume expansion of the fuel, stressing the clad at several places. This could have led to the formation of incipient cracks in the cladding that grew by the delayed hydride cracking.

Typical failures observed in the other low burnup fuel bundles are shown in Fig. 14(a–d). The pin hole observed in Fig. 14(a) is caused by formation of a hydride blister on the active length of the fuel pin. The failure shown in Fig. 14(b) is caused by the damage to the bearing pad during fuelling operation. A typical hydride failure at the end cap weld is shown in Fig. 14(c–d). Such hydride induced failures have been completely eliminated by strict control of moisture inside the fuel pins.

#### 4.2.3. $\text{ThO}_2$ fuel bundle

The  $\text{ThO}_2$  fuel bundle irradiated in KAPS to a burnup of 11000  $\text{MWd/t(Th)}$  did not show any defect or aberration, as revealed by the results from leak test and visual examination of the individual pins after dismantling the bundle. Puncture tests carried out on the individual pins did not indicate any fission gas release. However, the gamma scanning carried out on the central fuel pin and the pins from the intermediate and the outer rings revealed distinctive difference in the relative counts of  $\text{Cs}^{137}$  between 19-element  $\text{UO}_2$  bundle and the  $\text{ThO}_2$  bundle, as shown in Fig. 15(a–b). In the case of  $\text{UO}_2$  bundle the relative count of  $\text{Cs}^{137}$  monotonically increased from the central pin to the outer pin. However, in  $\text{ThO}_2$  bundle maximum count of  $\text{Cs}^{137}$  was noticed

in the fuel pin from the intermediate ring, suggesting that the burnup is more in the intermediate pin due to the breeding of  $\text{U}^{233}$ .

#### 4.3. TAPS BWR fuel [10,11]

Nodular corrosion was the predominant feature noticed on the fuel clad of TAPS fuel pins as shown in Fig. 16. The concentration of corrosion nodules in the fuel elements followed the burnup profile, the concentration being higher in regions of higher burnup. However, nodular corrosion was limited only to the initial-load-design-fuel and was not observed in the subsequent reload-design-fuel.

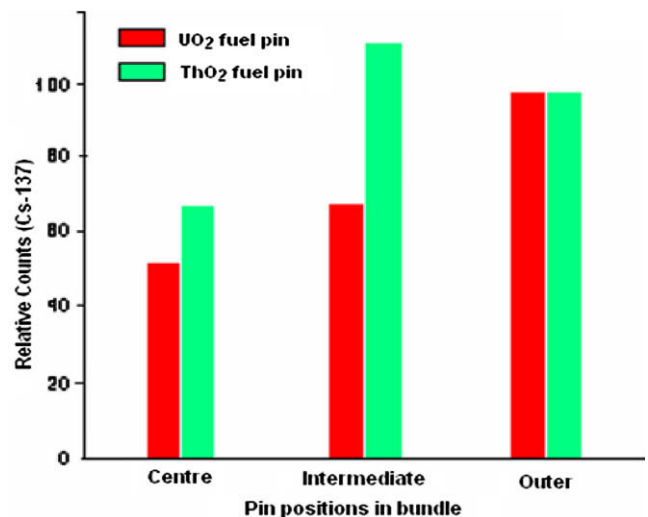


Fig. 15. Relative  $\text{Cs}^{137}$  distribution between the centre, middle and outer pins in  $\text{UO}_2$  fuel and in  $\text{ThO}_2$  fuel.



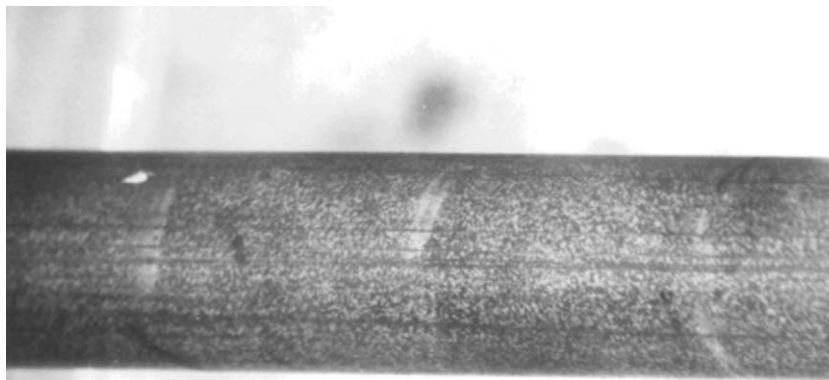


Fig. 16. Nodular corrosion observed on a TAPS fuel pin.

Fission gas release measurements were carried out by puncturing the intact fuel elements in the plenum region. It was observed that the measured gas releases varied from 1.0% to 13.6%. Three modes of fuel failure have been generally observed during the PIE of pins from TAPS namely, internal hydriding at the top end plug weld, fretting at a spacer grid site and pellet clad interaction induced stress corrosion cracking (PCI/SCC) of the cladding [10].

## 5. Conclusions

The findings from the post irradiation examination of different fuels are as follows:

1.  $\text{UO}_2$ –4% $\text{PuO}_2$  mixed oxide fuel clusters had performed well during experimental irradiation up to a burnup of 16000 MWd/tU. The fuel irradiated up to a peak linear heat rating of 414 W/cm had a lower fission gas release (<1%), compared to the fuel irradiated at a peak linear heat rating of 490 W/cm (8–10%).
2. PHWR fuel bundle irradiated to extended burnup performed very well under normal operating conditions. No abnormal corrosion or PCI was observed. However, the fission gas pressure in the outer fuel elements of fuel bundle was in the range of 21–28 bar at ambient temperature, higher compared to the pressure in the fuel elements from the intermediate and the central rings (3.2 and 4.4 bar). Suitable design modifications may be required to take care of this if the design burnup is to be extended.
3. The  $\text{ThO}_2$  fuel bundle irradiated to a burnup of 11000 MWd/t(Th) showed excellent performance and did not show any defect or aberration. No fission gas release was noticed.
4. In  $\text{ThO}_2$  fuel bundle, the burnup of the fuel from the intermediate ring was found to be higher than that of the outer ring. This could be due to the higher rate of breeding and subsequent burning of the fissile isotope  $\text{U}^{233}$  in the intermediate ring as compared to the outer ring.
5. The main causes of failures in the fuel pins of power reactors were identified as weld defects, hydriding and PCI. These failures have been eliminated by stringent quality control of welds,

strict control of moisture and other hydrogenous substances inside fuel pins and graphite lubrication of inside surface of cladding tube.

## Acknowledgement

The authors express their gratitude to all the colleagues in Post Irradiation Examination Division for their assistance in carrying out the experiments.

## References

- [1] K.S. Sivaramakrishnan, J.K. Bahl, K.C. Sahoo, S. Chatterjee, D.N. Sah, Radiometallurgy hot cells at BARC, Trombay, B.A.R.C/I-425, Bhabha Atomic Research Centre, Mumbai, 1976.
- [2] S. Chatterjee, Kamlesh Pandit, E. Ramadasan, S. Anantharaman, Anil Bhandekar, D.N. Sah, New hot cells facility at PIE division, Internal report, PIE division, Bhabha Atomic Research Centre, Mumbai, January 2007.
- [3] P.R. Roy, D.S.C. Purushotham, S. Majumdar, R. Ramachandran, H.S. Kamath, J.K. Ghosh, G.L. Goswami, Arun Kumar, K.N. Kedia, K.V.J. Asari, V.R. Nair, M.R. Nair, P.P. Rajagopalan, M.N.B. Pillai, O.L. D'Souza, Fabrication of MOX fuel element clusters for irradiation in PWL, CIRUS, B.A.R.C-1203, Bhabha Atomic Research Centre, Mumbai, 1983.
- [4] U. K. Viswanathan, S. Anantharaman, K.C. Sahoo, Measurement of fission gas release from irradiated nuclear fuel elements, B.A.R.C/2005/E/026, Bhabha Atomic Research Centre, Mumbai, 2005.
- [5] D.N. Sah, U.K. Viswanathan, K. Unnikrishnan, Prerna Mishra, R.S. Shrivastaw, S. Anantharaman, Post-irradiation examination of high burn-up PHWR fuel bundle 56504 from KAPS-1, B.A.R.C/2007/E/002, Bhabha Atomic Research Centre, Mumbai, 2007.
- [6] D.R. Olander, Fundamental aspects of nuclear reactor fuel elements, TID 26711-P1, 1976.
- [7] K. Unnikrishnan, E. Ramadasan, Microstructural changes in the fuel of TAPS during irradiation, in: Proceedings of Symposium on Radiation Effects in Solids, November 23–25, Bhabha Atomic Research Centre, Mumbai, 1983, p. 221.
- [8] D.N. Sah, Met. Mater. Process. 18 (1) (2006) 27.
- [9] Prerna Mishra, K. Unnikrishnan, U.K. Viswanathan, R.S. Shrivastaw, J.L. Singh, P.M. Ouseph, V.D. Alur, H.N. Singh, S. Anantharaman, D.N. Sah, Post irradiation examination of a failed PHWR fuel bundle from KAPS-2, B.A.R.C/2006/E/019, Bhabha Atomic Research Centre, Mumbai, 2006.
- [10] J.K. Bahl, D.N. Sah, S. Chatterjee, K.S. Sivaramakrishnan, Post irradiation examination of fuel elements of TAPS, Report B.A.R.C-1014, Bhabha Atomic Research Centre, Mumbai, 1979.
- [11] K.C. Sahoo, Post irradiation examination of thermal reactor fuels, PIENUP-89, in: Proceedings of Symposium on Post Irradiation Examination in Nuclear Programme, November 29–December 1, Bhabha Atomic Research Centre, Mumbai, vol. 1, 1989.